

Glacier shrinkage in the Alps continues unabated as revealed by a new glacier inventory from Sentinel-2

Frank Paul¹, Philipp Rastner¹, Roberto Sergio Azzoni², Guglielmina Diolaiuti², Davide Fugazza², Raymond Le Bris¹, Johanna Nemeč³, Antoine Rabatel⁴, Mélanie Ramusovic⁴, Gabriele Schwaizer³, Claudio Smiraglia²

¹ Department of Geography, University of Zurich, Zurich, Switzerland

² Department of Environmental Science and Policy, University of Milan, Milan, Italy

³ ENVEO IT GmbH, Innsbruck, Austria

⁴ Univ. Grenoble Alpes, CNRS, IRD, Grenoble-INP, Institut des Géosciences de l'Environnement (IGE, UMR5001), Grenoble, France

Correspondence: Frank Paul (frank.paul@geo.uzh.ch)

Abstract

The on-going glacier shrinkage in the Alps requires frequent updates of glacier outlines to provide an accurate database for monitoring, modeling purposes (e.g. determination of run-off, mass balance, or future glacier extent) and other applications. With the launch of the first Sentinel-2 (S2) satellite in 2015, it became possible to create a consistent, Alpine-wide glacier inventory with an unprecedented spatial resolution of 10 m. Already the first S2 images from August 2015 provided excellent mapping conditions for most glacierised regions in the Alps and were used as a base for the compilation of a new Alpine-wide glacier inventory in a collaborative team effort. In all countries, glacier outlines from the latest national inventories have been used as a guide to compile an update consistent with the respective previous interpretation. The automated mapping of clean glacier ice was straightforward using the band ratio method, but the numerous debris-covered glaciers required intense manual editing. Cloud cover over many glaciers in Italy required including also S2 scenes from 2016. The outline uncertainty was determined with multiple digitising of 14 glaciers by all participants. Topographic information for all glaciers was obtained from the ALOS AW3D30 DEM. Overall, we derived a total glacier area of $1806 \pm 60 \text{ km}^2$ when considering 4395 glaciers $>0.01 \text{ km}^2$. This is 14% (-1.2%/a) less than the 2100 km^2 derived from Landsat in 2003 and indicating an unabated continuation of glacier shrinkage in the Alps since the mid-1980s. It is a lower bound estimate, as due to the higher spatial resolution of S2 many small glaciers were additionally mapped or they increased in size compared to 2003. Median elevations peak around 3000 m a.s.l. with a high variability that depends on location and aspect. The uncertainty assessment revealed locally strong differences in interpretation of debris-covered glaciers, resulting in limitations for change assessment when using glacier extents digitised by different analysts. The inventory is available at: [doi.pangaea.de/10.1594/PANGAEA.909133](https://doi.org/10.1594/PANGAEA.909133) (Paul et al., 2019).

39 **1. Introduction**

40 Information on glacier extents is required for numerous glaciological and hydrological calculations,
41 ranging from the determination of glacier volume, surface mass balance and future glacier evolution to
42 run-off, hydro-power production, and sea-level rise (e.g., Marzeion et al., 2017). For these and several
43 other applications glacier outlines spatially constrain all calculations thus providing an important base-
44 line dataset. In response to the on-going atmospheric warming, glaciers retreat, shrink and lose mass in
45 most regions of the world (e.g., Gardner et al. 2013, Wouters et al. 2019, Zemp et al. 2019). Accord-
46 ingly, a frequent update of glacier inventories is required to reduce uncertainties in subsequent calcula-
47 tions. With relative area loss rates of about 1% per year in many regions globally (Vaughan et al.
48 2013), glaciers lose about 10% of their area within a decade and a decadal update frequency seems
49 sensible. In regions with stronger glacier shrinkage such as the tropical Andes (e.g. Rabatel et al. 2013,
50 2018) or the European Alps (e.g. Gardent et al. 2014) an even higher update frequency is likely re-
51 quired. However, apart from the high workload required to digitise or manually correct glacier outlines
52 (e.g. Racoviteanu et al. 2009), it is often not possible to obtain satellite images in a desired period of
53 the year with appropriate mapping conditions, i.e. without seasonal snow and clouds hiding glaciers.
54 Hence, glacier inventories are often compiled from images acquired over several years resulting in a
55 temporarily inhomogeneous dataset. Fortunately, a 3-year period of acquisition is still acceptable in
56 error terms, as area changes of about $\pm 3\%$ are within the typical area uncertainty of about 3 to 5% (e.g.
57 Paul et al. 2013).

58

59 The last glacier inventory covering the entire Alps with a common and homogeneous date was com-
60 piled from Landsat Thematic Mapper (TM) images acquired within six weeks in the summer of 2003
61 (Paul et al. 2011). Although this dataset has its caveats (e.g. missing small glaciers in Italy and some
62 debris-covered ice), it is methodologically and temporarily consistent and represents glacier outlines
63 of the Alps in the Randolph Glacier Inventory (RGI). A few years later, high quality glacier invento-
64 ries were compiled from better resolved datasets (aerial photography, airborne laser scanning) on a
65 national level in all four countries of the Alps with substantial glacier coverage (Austria, France, Italy,
66 Switzerland). These more recent inventories refer to the periods 2008-2011 for Switzerland (Fischer et
67 al. 2014), 2004-2011 for Austria (Fischer et al. 2015), 2006-2009 for France (Gardent et al. 2014), and
68 2005-2011 for Italy (Smiraglia et al. 2015). As an 8-year period is rather long, consistent and compa-
69 rable change assessment is challenging. However, for the first version of the World Glacier Inventory
70 (WGI) the temporal spread was even larger, ranging from 1959 to about 1983 (Zemp et al. 2008). An-
71 other problem for change assessment is the inhomogenous interpretation of glacier extents that occurs
72 in part to be compliant with the interpretation in earlier national inventories. Hence, calculations over
73 the entire Alps that require a consistent time stamp are difficult to perform and rates of glacier change
74 are difficult to compare across regions (e.g. Gardent et al. 2014).

75

76 Considering the on-going strong glacier shrinkage in the Alps over the past decades and the above
77 shortcomings of existing datasets, there is a high demand to compile a (1) new, (2) precise and (3)
78 consistent glacier inventory for the entire Alps, with data acquired under (4) good mapping conditions
79 in (5) a single year. Although it might be difficult to satisfy all five criteria at the same time, at least
80 some of them seem achievable by means of recently available satellite data. With the 10 m resolution
81 data from Sentinel-2 (S2) and its 290 km swath width it is possible (a) to improve the quality of the
82 derived glacier outlines (compared to Landsat TM) substantially (Paul et al. 2016) and (b) to cover a
83 region such as the Alps with a few scenes acquired within a few weeks or even days, satisfying criteria
84 (2) and (5). Good mapping conditions, however, only occur by chance after a comparably warm sum-
85 mer when all seasonal snow off glaciers has melted and largely cloud free conditions persist over an
86 extended time span in August or September.

87

88 We here present a new glacier inventory for the European Alps that has been compiled from S2 data
89 that were mostly acquired within two weeks of August 2015 (during the commissioning phase). How-
90 ever, due to glaciers (mostly in Italy) being partly cloud-covered, also scenes from 2016 (and very few
91 from 2017) were used. Hence, criterion (5) could not be fully satisfied. In order to satisfy point (3), we
92 decided to perform the mapping of clean ice with an identical method (band ratio), and distribute the
93 raw outlines to the national experts for editing of wrongly classified regions (e.g. adding missing ice in
94 shadow and under local clouds or debris cover, removing lakes and other water surfaces). As a guide
95 for the interpretation the analysts used the latest high-resolution inventory in each country. All cor-
96 rected datasets were merged into one dataset and topographic information for each glacier was derived
97 from the ALOS AW3D30 DEM. For uncertainty assessment all five participants corrected the extents
98 of 14 glaciers independently four times.

99

100 **2. Study region**

101 The Alps are a largely west-east (south-north in the West) oriented mountain range in the centre of
102 Europe (roughly from 2° to 18° E and 43° to 49° N) with peaks reaching 4808 m a.s.l. in the West at
103 Mt. Blanc/Monte Bianco and elevations above 3000 m a.s.l. in most regions. In Fig. 1 we show the
104 region covered by glaciers along with footprints of the tiles used for data processing. The Alps act thus
105 as a topographic barrier for air masses coming from the North and South (Auer et al. 2007) as well as
106 from the West in the western part. This results in enhanced orographic precipitation and a high region-
107 al variability of precipitation amounts in specific years as well as in the long-term mean (e.g. Frei et al.
108 2003). On the other hand, temperatures are horizontally rather uniform (e.g. Böhm et al. 2001) but
109 vary strongly with height according to the atmospheric lapse rate (e.g. Frei 2014). Snow accumulation
110 is mostly due to winter precipitation, but some snowfall can also occur in summer at higher elevations,
111 reducing ablation for a few days.

112

113 There is no significant long-term trend in precipitation over the last 100+ years (Casty et al. 2005), but
114 summer temperatures in the Alps have increased sharply (by about 1 °C) in the mid-1980s (e.g. Benis-
115 ton 1997, Reid et al. 2016). In consequence, winter snow cover barely survives the summer even at
116 high elevations and / or when strong positive deviations in temperature occurred. Glacier mass balanc-
117 es in the Alps were thus pre-dominantly negative over the past three decades (e.g. Zemp et al. 2015)
118 and the related mass loss resulted in widespread glacier shrinkage and disintegration over the past dec-
119 ades (e.g. Gardent et al. 2014, Paul et al. 2004). An order of magnitude estimate with a rounded total
120 area of about 2000 km² in 2003 and a mean annual specific mass loss of 1 m w.e. per year (e.g. Zemp
121 et al. 2015), gives a loss of about 2 Gt of ice per year in the Alps.

122

123 Most glaciers in the Alps are of cirque, mountain and valley type and the two largest ones (Aletsch
124 and Gorner glaciers) have an area of about 80 km² and 60 km², respectively. Some glaciers reach down
125 to 1300 m a.s.l., and the overall mean elevation is around 3000 m a.s.l., a unique value compared to
126 other regions of the RGI (e.g. Pfeffer et al. 2014). Due to the surrounding often ice-free rock walls of
127 considerable height, many glaciers in the Alps are heavily debris-covered. Whereas this allowed the
128 tongues of several large valley glaciers to survive at comparably low elevations (Mölg et al. 2019),
129 many glaciers - large and small - become hidden under increasing amounts of debris. Combined with
130 the on-going down-wasting and disintegration, precisely mapping their extents is increasingly chal-
131 lenging.

132

133

134

Figure 1

135 **3. Datasets**

136 **3.1 Satellite data**

137 We processed 17 different S2 tiles from a total of eight different dates to cover the study region with
138 cloud free images (Figure 1 and Table 1). These are split among the 4 countries resulting in 29 inde-
139 pendently processed image footprints. Of these, 15 were acquired in 2015, 11 in 2016 and 3 in 2017.
140 Convective clouds in Italy (mostly along the Alpine main divide) required extending the main acquisi-
141 tion period over two years. All glaciers in France were mapped from four tiles acquired on 29.8.2015.
142 This date covers also most glaciers mapped in Switzerland (five tiles) apart from the south-east tile
143 32TNS (ID: 11) that was acquired three days earlier (26.8.2015). Two tiles from that date
144 (32TNT/TPT) are used to map glaciers in western-Austria and three tiles (32TQT/TQS and 33TUN)
145 from 27.8.2016 for the eastern part of Austria. Twelve tiles cover the glaciers in Italy, seven from
146 2016 and in total five from 2015 and 2017 (Fig. 1). However, those from 2017 only cover very few
147 and small glaciers so that collectively the northern (Switzerland / Austria) and western (France) parts
148 of the inventory are from 2015 whereas the southern (Italy) and eastern (Austria) parts are from 2016.
149 All tiles were downloaded from remotepixel.ca (only the required bands, this is no longer possible),

150 earthexplorer.usgs.gov or the Copernicus Hub.

151

152 *Table 1*

153

154 From all tiles, bands 2, 3, 4, 8, and 11 (blue, green, red, Near Infra-Red / NIR, Short Wave Infra-Red /
155 SWIR) of the sensor Multi Spectral Imager (MSI) were downloaded and colour composites were cre-
156 ated from the 10 m visible and NIR (VNIR) bands. The 20 m SWIR band 11 was bilinearly resampled
157 to 10 m resolution to obtain glacier outlines at this resolution. The 10 m resolution VNIR bands al-
158 lowed for a much better identification of glacier extents (e.g. correcting debris-covered parts) than
159 possible with Landsat (Paul et al. 2016), resulting in a higher quality of the outlines. Apart from the
160 resampling, all image bands are used as they are except for Austria, where further pre-processing has
161 been applied (see Section 4.2.1). The August 2015 scenes from the S2 commissioning phase had re-
162 flectance values stretched from 1 to 1000 (12 bit) instead of the later 16 bit (allowing values up to
163 65536), but this linear rescaling had no impact on the threshold value for the band ratio (see Section
164 4.1).

165

166 **3.2 Digital elevation models (DEMs)**

167 We originally intended using the new TanDEM-X (TDX) DEM to derive topographic information for
168 all glaciers, as it covers the entire Alps and was acquired closest (around 2013) to the satellite images
169 used to create the inventory. However, closer inspection revealed that it had data voids and suffered
170 from artefacts (Fig. 2). Although these are mostly located in the steep terrain outside of glaciers, many
171 smaller glaciers are severely impacted, resulting in wrong topographic information. As an alternative
172 we investigated the ALOS AW3D30 DEM that was compiled from ALOS tri-stereo scenes (Takaku et
173 al. 2014) and acquired about five years before the TDX DEM (around 2008). The AW3D30 DEM has
174 a less good temporal match but no data voids and comparably few artefacts (Fig. 2). The individual
175 tiles were merged into one 30 m dataset in UTM 32N projection with WGS84 datum. For the pre-
176 processing of satellite bands in Austria, a national DEM with 10 m resolution derived from laser scan-
177 ning was used (Open Data Österreich: data.gv.at).

178

179 *Figure 2*

180

181 **3.3 Previous glacier inventories**

182 Outlines from previous national glacier inventories were used to guide the delineation. They have been
183 mostly compiled from aerial photography with a spatial resolution better than 1 m and should thus
184 provide the highest possible quality. This allowed considering very small and otherwise unnoticed
185 glaciers and helped to identify glacier zones that are debris covered. The substantial glacier retreat that
186 took place between the two inventories was well visible in most cases and did not hamper the interpre-
187 tation. However, a larger number of mostly very small glaciers were either not mapped in 2003 and
188 have now been added or they were smaller in 2003 and have now larger extents. A large issue with

189 respect to additional work load is the compilation of ice divides. They can be derived semi-
190 automatically from watershed analysis of a DEM using a range of methods (e.g. Kienholz et al. 2013),
191 but in general many manual corrections have still to be applied. To have consistency with previous
192 national inventories, we decided to use the drainage divides from these inventories to separate glacier
193 complexes into entities. However, due to the locally poor geolocation of S2 scenes in steep terrain
194 (Kääb et al. 2016, Stumpf et al. 2018) some ice divides of the former inventories overlapped with glacier
195 extents (by up to 50 m) and were manually adjusted.

196

197 **4. Methods**

198 **4.1 Mapping of clean ice in all regions**

199 Automated mapping of clean to slightly dirty glacier ice is straightforward using a red or NIR to
200 SWIR band ratio and a (manually selected) threshold (e.g. Paul et al. 2002). Also other methods such
201 as the normalised difference snow index (NDSI) work well (e.g. Racoviteanu et al. 2009) as both uti-
202 lise the strong difference in reflectance from the VNIR to the SWIR for snow and ice (e.g. Dozier
203 1989). As the latter are bright in the VNIR bands (high reflectance) but very dark (low reflectance) in
204 the SWIR, dividing a VNIR band by a SWIR band gives high values over glacier ice and snow and
205 very low ones over all other terrain as this is often much brighter in the SWIR than the VNIR. The
206 manual selection of a threshold for each scene (or S2 tile) has the advantage to include a regional ad-
207 justment of the threshold to local atmospheric conditions. We followed the recommendation to select
208 the threshold in a way that good mapping results in regions with shadow are achieved. By lowering the
209 threshold, more and more rock in shadow is included, creating a noisy result. It has been shown by
210 Paul et al. (2016) that glacier mapping with S2 (using a red / SWIR ratio) requires an additional
211 threshold in the blue band to remove misclassified rock in shadow (that can have the same ratio value
212 as ice in shadow but is darker in the blue band). Hence, for this inventory glaciers have been first au-
213 tomatically identified following the equation:

214

$$215 \quad (\text{red} / \text{SWIR}) > th_1 \text{ and blue} > th_2$$

216

217 with the empirically derived thresholds th_1 and th_2 . As mentioned above, the SWIR band was bilinear-
218 ly resampled from 20 to 10 m spatial resolution before computing the ratio. No filter for image
219 smoothing was applied to retain fine spatial details, such as rock outcrops. Figure 3 shows for a test
220 site in the Mt. Blanc region (Leschaux Glacier) the impact of the threshold selection. Figure 3a depicts
221 the (contrast stretched) red / SWIR ratio image, Fig. 3b the impact of th_1 on the mapped area, Fig. 3c
222 the impact of th_2 , and Fig. 3d the resulting outlines after raster-vector conversion. As can be seen in
223 Fig. 3b, there is very little impact on the mapped glacier area when increasing th_1 in steps of 0.2. For
224 this region we used 3.0 as th_1 resulting in the blue and yellow areas as the mapped glacier. Wrongly
225 mapped rock in shadow is then reduced back with th_2 (Fig. 3c) that is selected by visual analysis and

226 expert judgment. In this case a value of 860 was selected for th_2 i.e. only the blue area in Fig. 3c is
227 considered. This removed rock in shadow from the glacier mask for the region to the right of the white
228 arrow but, on the other hand, correctly mapped ice in shadow is removed at the same time in the re-
229 gion above the green arrow (Figs. 3c and d). Hence, threshold selection is always a compromise as it is
230 in general not possible to map everything correctly with one set of thresholds. In the resulting binary
231 glacier maps the ‘non-glacier’ class is set to ‘no data’ before they were converted to a shape file using
232 raster-vector conversion. In the resulting shape file internal rocks are thus data voids.

233

234 All pre-processed scenes were provided in their original geometry for correction by the national ex-
235 perts. As shown in Fig. 3c, it was sometimes not possible to include dark bare ice and at the same time
236 exclude bare rock in shadow. Such wrongly classified regions were corrected by the analysts together
237 with data gaps for debris cover and clouds (omission errors), wrongly mapped water bodies (e.g. tur-
238 bid lakes and rivers) and shadow regions (commission errors). By setting the minimum glaciers size to
239 0.01 km^2 , most of the often very small snow patches (i.e. $<0.01 \text{ km}^2$) were removed (cf. Leigh et al.
240 2019).

241

242

Figure 3

243

244 **4.2 Corrections in the different countries**

245 **4.2.1 Austria**

246 The satellite scenes for Austria were further pre-processed by G. Schwaizer (cf. Paul et al. 2016) to
247 remove water surfaces and improve classification of glacier ice in cast shadow, before manual correc-
248 tions were applied. The latter work was mainly performed by one person (J. Nemeč). Two previous
249 Austrian glacier inventories (Lambrecht and Kuhn 2007, Fischer et al. 2015) were used to support the
250 interpretation of small glaciers, debris covered glacier parts, and the boundary across common accu-
251 mulation areas. Further, an internal independent quality control of the generated glacier outlines was
252 made by a second person (G. Schwaizer), using orthophotos (30 cm resolution) acquired in late Au-
253 gust 2015 for most Austrian glaciers for overall accuracy checks and to assure the correct delineation
254 of debris covered glacier areas. In Fig. 4a we illustrate the strong glacier shrinkage from 1998 (yellow
255 lines) to 2016 (red) as well as the manual corrections applied, extending the bright filled areas of the
256 raw classification to the red extents.

257

258 **4.2.2 France**

259 The raw glacier outlines from S2 were corrected by one person (A. Rabatel). The glacier outlines from
260 the previous inventory by Gardent et al. (2014) were used for the interpretation, in particular in shad-
261 ow regions and for glaciers under debris cover. It is noteworthy that the previous inventory was made
262 on the basis of aerial photographs (2006-2009) with field campaigns for the debris-covered glacier
263 tongues to clarify the outline delineation. As a consequence, this previous inventory constitutes a high-
264 ly valuable reference. In addition, because even on debris-covered glaciers the changes between 2006-

265 09 and 2015 are visible (Fig. 4b), Pléiades images from 2015-2016 acquired within the KALIDEOS-
266 Alpes / CNES program were use as a guideline, mostly for the heavily debris-covered glacier tongues.

267

268 **4.2.3 Italy**

269 As mentioned above, clouds covered the southern Alpine sector on the S2 scenes from August 2015.
270 Hence, most of the inventory was compiled based on images from 2016 and three scenes from 2017
271 (see Table 1) were used to map glaciers under clouds or with adverse mapping conditions, i.e. exces-
272 sive snow cover or shadows in the other scenes. Images acquired in August 2016 had little residual
273 seasonal snow and a high solar elevation at the time of acquisition, which minimised shadow areas
274 creating very good mapping conditions. In September 2016 and October 2017, more snow was present
275 on high mountain cirques and glacier tongues, but comparatively few snow patches were found out-
276 side glaciers. However, the lower solar elevation compared to August caused a few north-facing glaci-
277 ers and glacier accumulation areas to be under shadows. The raw glacier outlines from S2 were cor-
278 rected by two analysts (D. Fugazza, R.S. Azzoni). The outlines were separated into regions based on
279 the administrative division of Italy, following the previous Italian glacier inventory (Smiraglia et al.
280 2015).

281

282 Seasonal snow and rocks in shadow that were wrongly identified as clean ice were manually deleted
283 by the analysts, as well as lakes and large rivers. In shadow regions, and for glaciers with large debris
284 cover, the outlines from the previous Italian inventory by Smiraglia et al. (2015) were particularly val-
285 uable as a guide. Where some small glaciers were entirely under shadows, the outlines from the previ-
286 ous inventory were copied without changes, while in case of partial shadow coverage they were edited
287 in their visible portions. Due to the comparably small area changes of such glaciers over time, the
288 former outlines are likely more precise than a new digitization under such conditions (cf. Fischer et al.
289 2014).

290

291 Glaciers in the Orobic Alps (ID 12 in Fig. 1), Dolomites and Julian Alps (ID 18) posed significant
292 challenges for glacier mapping. The three regions host very small niche glaciers and glacierets: in the
293 Orobic and Julian Alps, their survival is granted by abundant snow-falls, northerly aspect and accumu-
294 lation from avalanches, with debris cover also playing an important role. In the Dolomites, debris cov-
295 er is often complete (Smiraglia and Diolaiuti 2015), while the steep rock walls provide shadow and
296 further complicate mapping. For glaciers in the Orobic Alps, an aerial orthophoto acquired by Regione
297 Lombardia (geoportale.regione.lombardia.it) in 2015 was used to aid the interpretation in view of its
298 finer spatial resolution (e.g. Fischer et al. 2014, Leigh et al. 2019), although the image also shows evi-
299 dence of seasonal snow. Here, manual delineation of the glacier outlines was required as the band ratio
300 approach could only detect small snow patches (see Fig. 4c). In the other two regions, outlines from
301 the previous inventory, derived from aerial orthophotos acquired in 2011, were copied and only cor-
302 rected where evidence of glacier retreat was found. Whereas the uncertainty in the outlines of the latter

303 glaciers can be large (some of them are marked as ‘extinct’ in the first Italian inventory from 1959 to
304 1962), the combined glacier area from the three regions is just above 1% (1.35 km²) of the total area of
305 Italian glaciers. For several of these very small, partly hidden entities one can certainly discuss if they
306 should be kept at all. In this inventory, they have been included for consistency with the last national
307 inventory.

308

309 **4.2.4 Switzerland**

310 The raw glacier outlines from S2 were corrected by three persons (R. LeBris, F. Paul, P. Rastner) each
311 of them being responsible for a different main region (south of Rhone, north of Rhone/Rhine, south of
312 Rhine). The glacier outlines from the previous inventory by Fischer et al. (2014) were highly valuable
313 for the interpretation, in particular in shadow regions and for glaciers under debris cover. In the hot
314 summer of 2015 most seasonal snow had disappeared by the end of August so that mapping conditions
315 with a comparably high solar elevation (limited regions in shadow) were very good. Some glaciers that
316 could not be identified in the (contrast-stretched) S2 images were either copied from the previous in-
317 ventory (if located in shadow) or assumed to have disappeared (if sun-lit). Wrongly mapped (turbid)
318 lakes and rivers (Rhone, Aare) were manually removed.

319

320 In a few cases (mostly debris-covered glaciers) we had to deviate from the interpretation of the previ-
321 ous inventories. As shown in Fig. 4d, very high-resolution satellite imagery or aerial photography (as
322 available in Google Earth or from map servers) do not always help for a ‘correct’ interpretation of
323 glacier extents, as the rules applied for identification of ice under debris cover might differ (see Figs.
324 S1, S2 and S3 in the Supplement). In this case it seems that the debris-covered region was not correct-
325 ed in the 2003 and 2008 inventories, but is now included (one can still discuss the boundaries). The
326 interpreted glacier area has thus strongly grown since 2003 due to the better visibility of debris cover
327 with S2.

328

329

Figure 4

330

331 **4.3. Drainage divides and topographic information**

332 Drainage divides between glaciers were copied from previous national inventories but were locally
333 adjusted along national boundaries. In part this was required because different DEMs had been used in
334 each country to determine the location of the divide. Additionally, some glaciers are divided by na-
335 tional boundaries rather than flow divides. This can result in an arbitrary part of the glacier (e.g. its
336 accumulation zone) being located in one country and the other part (e.g. its ablation zone) in another
337 country. As this makes no sense from a glaciological (and hydrological) point of view, such glaciers
338 (e.g. Hochjochferner in the Ötztal Alps) have been corrected in a way that they belong to the country
339 where the terminus is located. There are thus a few inconsistencies in this inventory compared to the
340 national ones.

341

342 After digital intersection of glacier outlines with drainage divides, topographic information for each
343 glacier entity is calculated from both DEMs (ALOS and TDX) following Paul et al. (2009). The calcu-
344 lation is fully automated and applies the concept of zone statistics introduced by Paul et al. (2002).
345 Each region with a common ID (this includes regenerated glaciers consisting of two polygons) is in-
346 terpreted as a zone over which statistical information (e.g. minimum / maximum / mean elevation) is
347 derived from an underlying value grid (e.g. a DEM or a DEM-derived slope and aspect grid). Apart
348 from glacier area (in km²) all glaciers have information about mean, median, maximum and minimum
349 elevations, mean slope and aspect (both in degrees) and aspect sector (eight cardinal directions) using
350 letters and numbers (N=1, NE=2, etc.). Further information appended to each glacier in the attribute
351 table of the shape file is the satellite tile used, the acquisition date, the analyst and the funding source.
352 This information is applied automatically by digital intersection (*'spatial join'*) to all glaciers from a
353 manually corrected scene footprint shape file (see Fig. 1). The various attributes have then been used
354 for displaying key characteristics of the datasets in bar graphs, scatter plots and maps (see Section
355 5.1).

356

357 **4.4 Change assessment**

358 Glacier area changes have only been calculated with respect to the inventory from 2003, as the dates
359 for the previous national inventories were too diverse for a meaningful assessment (see Introduction).
360 To obtain consistent changes, only glaciers that are also mapped in the 2003 inventory are used for a
361 direct comparison (automatically selected via a *'point in polygon'* check). However, after realising that
362 a glacier-specific comparison is not possible due to differences in interpretation (caused by the higher
363 resolution of S2 and the different national rules) and changes in topology (e.g. inclusion of tributaries
364 that were separated in 2003), we decided to only compare the total glacier area of the previous and
365 new inventory.

366

367 **4.5 Uncertainty assessment**

368 As several analysts have digitised the new inventory, we decided performing multiple digitising of a
369 pre-selected set of glaciers to determine internal variability in interpretation per participant and across
370 participants as a measure of the uncertainty of the generated dataset. For this purpose, all participants
371 used the same raw outlines from S2 tile 32TLR to manually correct 14 glaciers (sizes from 0.1 to 10
372 km²) to the south of Lac des Dix around Mt. Blanc de Cheilon (3870 m a.s.l.) for debris cover. All
373 glaciers were digitised 4 times by 5 participants giving a nominal total of 280 outlines for comparison.
374 Results were analysed using an overlay of outlines to identify the general deviations in interpretation
375 and through a glacier-by-glacier comparison of glacier sizes. For the latter all datasets were intersected
376 with the same drainage divides and glacier-specific areas were calculated. For each glacier and the
377 entire region, mean area values and standard deviations are calculated per glacier, per participant and
378 for the total sample. The participants were asked to only use the S2 image and the 2003 outlines as a
379 guide for interpretation in the first two digitisation rounds and consider interpretation of very high-

380 resolution imagery as provided by Google Earth for the second two rounds. At a minimum, one day
381 should have passed between each digitisation round and it was not allowed to show any of the former
382 outlines. On average, each digitisation round took about 2 hours.

383
384 Additionally, we applied the buffer method (e.g. Paul et al. 2017) to obtain a statistical uncertainty
385 value for the entire sample. This method gives a minimum and maximum area and was used to deter-
386 mine a relative area difference. This value multiplied by 0.68 gives the standard deviation (assuming
387 normally distributed deviations from the correct outline) that is used as a further measure of area un-
388 certainty (Paul et al. 2017). The selected buffer is based on an earlier multiple digitising experiment
389 for a couple of glaciers (Paul et al. 2013) showing that the variability in the positioning is within one
390 pixel (or about ± 10 m in the current case) to both sides of the ‘true’ vector line. Strictly, a larger buffer
391 should be used for the debris-covered glacier parts, as their uncertainty is higher. However, we have
392 not implemented this here, as the related calculations are computationally expensive (cf. Mölg et al.
393 2018) and would still not reflect the real problem in debris identification as shown in Fig. 4d. Instead,
394 we additionally applied a ± 2 pixels buffer to all glaciers. For the majority of the debris-covered glaci-
395 ers (i.e. those where debris can at least be identified) this gives an upper bound value of the uncertain-
396 ty. Depending on the degree of debris cover along the perimeter, the uncertainty is between the two
397 values derived from the two buffers.

398

399 **5. Results**

400 **5.1 The new glacier inventory**

401 In total, we identified 4395 glaciers larger than 0.01 km^2 covering a total area of 1805.9 km^2 , of which
402 361.5 km^2 (20%) is found in Austria and 227.1 (12.6%), 325.3 (18%), and 892.1 km^2 (49.4%) in
403 France, Italy, and Switzerland, respectively. The size class distribution by area and count is depicted in
404 Fig. 5a and also listed in Table 2. In total, 62.5% (92%) of all glaciers are smaller than 0.1 km^2 (1.0
405 km^2) covering 5.5% (28%) of the glacierised area, whereas 1.6% are larger than 5 km^2 and cover 40%.
406 Thereby, glaciers in the size class 1 to 5 km^2 alone cover one third (31.5%) of the area but only 6.4%
407 of the total number. This biased size class distribution is typical for alpine glaciers where a few large
408 glaciers are surrounded by numerous much smaller ones. The distribution of glacier number and area
409 by aspect sector displayed in Fig. 5b shows the dominance, both in number and coverage area, of nor-
410 therly exposed glaciers compared to all other sectors. About 60% of all glaciers (covering 60% of the
411 area) are exposed to the NW, N, or NE whereas only 21% of all glaciers are found in the sectors SE, S,
412 and SW. This distribution of glacier aspects is typical for regions where radiation plays a larger role in
413 glacier existence compared to factors such as precipitation (Evans and Cox, 2005). The larger area
414 coverage for glaciers facing SE is mostly due to the large Aletsch and Fiescher glaciers.

415
416
417

Figure 5, Table 2

418 A plot of glacier surface area vs. minimum and maximum elevations (Fig. 6a) reveals that glaciers
419 smaller than 1 km² cover nearly the full range of possible elevations, indicating that their mean eleva-
420 tion is also impacted by factors other than climate (i.e. they can also exist at low elevations when they
421 are located in a well protected environment). Glaciers larger than 1 km² on the other hand have clearly
422 distinguished maximum and minimum elevations, i.e. they arrange around a climatically driven mean
423 elevation which is around 3000 m a.s.l. Plotting glacier area vs. elevation range (Fig. 6b) shows that
424 the largest glaciers are not those with the highest elevation range (the maximum of 3140 m is for Glac-
425 ier des Bossons in the Mont-Blanc massif with a size of 10 km²) and that for the majority of glaciers
426 the elevation range increases with glacier size. This is typical for regions dominated by mountain and
427 valley glaciers as these follow the given topography. The ca. 7 km² large Plaine Morte Glacier is a
428 plateau glacier with an elevation range of only 350 m and represents an exception from the rule that
429 larger glaciers have generally a larger elevation range.

430
431 *Figure 6*
432

433 The median elevation of a glacier is largely driven by temperature, precipitation and radiation receipt
434 (that depends on topography). As temperature is rather similar at the same elevation over large regions
435 (e.g. Zemp et al. 2007) and topography (aspect / shading) has a strong local impact on radiation re-
436 ceipt, the large-scale variability of median (or mean) elevation of a glacier has a high correlation with
437 precipitation (e.g. Ohmura et al. 1992, Oerlemans 2005, Rastner et al. 2012, Sakai et al. 2015). The
438 spatial distribution of glacier median elevations in the Alps (Fig. 7) thus also reflects the general pat-
439 tern of annual precipitation amounts (e.g. Frei et al. 2003). When focusing on glaciers larger than 0.5
440 km² (that are less impacted by local topographic conditions), clearly lower median elevations (around
441 2400 m a.s.l.) are found for glaciers along the northern margin of the Alps and major mountain passes
442 than in the inner Alpine valleys (around 3700 m a.s.l.) that are well shielded from precipitation. On top
443 of this variability comes the variability due to a different aspect (Fig. 7, inset): On average, glaciers
444 that are exposed to the south have median elevations that are about 250 m higher (mean 3125 m a.s.l.)
445 than north-facing glaciers (mean 2875 m a.s.l.). However, the scatter is high and for each aspect the
446 elevation variability is about 1500 m.

447
448 *Figure 7*
449

450 The graph in Fig. 8 shows the hypsometry of glacier area in the four countries and for the total area in
451 relative terms. On average, the highest area share is found around the mean elevation of 3000 m a.s.l.
452 By referring for each country to the total area as 100%, differences among them can be seen. Most
453 notable is the smaller elevation range and larger peak of glaciers in Austria, the broader vertical distri-
454 bution in Switzerland (with the lowest peak value), and the slightly higher peak of the distribution in
455 Italy (at 3100 m a.s.l.). The hypsometry of glaciers in France is closest to the curve for the entire Alps.

456
457 *Figure 8*

458

459 **5.2 Area changes**

460 For a selection of 2873 comparable polygon entities present in both inventories, total glacier area
461 shrunk from 2060 km² in 2003 to 1783 km² in 2015/16 or by -13.2% (-1.1%/a). Considering the as-
462 sumed missing area in the 2003 inventory of about 40 km² (glaciers with area gain are 29.4 km² larger
463 in 2015/16 than in 2003), a more realistic area loss is -15% or -1.3%/a. This is about the same pace as
464 reported earlier by Paul et al. (2004) for the Swiss Alps from 1985 to 1998/99 (-1.4%/a). An example
465 of the strong glacier shrinkage in Austria is depicted in Fig. 9. Closer inspection of this image also
466 reveals a small shift (about up to 50 m to the SE) of the S2 scenes compared to the earlier Landsat TM
467 scenes.

468

469

Figure 9

470

471 The comparison of glacier outlines in Fig. 10 illustrate for the region around Sonnblickkees in Austria
472 why we do not provide a scatterplot of relative area changes vs. glacier size or country specific area
473 change values (cf. also Fig. 4d for Gavirolas Glacier in Switzerland). Due to the different interpreta-
474 tions in the new inventory, 125 mostly very small glaciers are 100% to 630% larger than in 2003 and a
475 large number (557) is 0% to 100% larger. For example, the 4 km² Suldenferner has increased in size
476 by 550% as a small tributary (that holds the ID for the glacier) was disconnected in 2003 but is now
477 connected to the entire glacier. Although such cases can be manually adjusted, it would not solve the
478 general problem of the different interpretation when using data sources with differing spatial resolu-
479 tion (cf. Fischer et al. 2014, Leigh et al. 2019). For example, the glacier in Fig. 4d has increased its
480 size from 2003 to 2015 by 56% due to the new interpretation. On the other hand, Careser glacier,
481 which fragmented in six ice bodies from 2003 to 2015, lost 55% of its area when summing up all parts
482 as opposed to 63% when considering the largest glacier only. In consequence, the possible area reduc-
483 tion due to melting is partly compensated by the more generous interpretation of glacier extents and
484 thus with a limited meaning on the basis of individual glaciers. Overall, glacier extents in the 2015/16
485 inventory might be somewhat larger than in reality due to the inclusion of seasonal/perennial snow in
486 some regions. The -15% area loss mentioned above can thus be seen as a lower bound estimate.

487

488

Figure 10

489

490 **5.3 Uncertainties**

491 **5.3.1 Glacier outlines**

492 The multiple digitising experiment revealed several interesting albeit well-known results. Overall, the
493 area uncertainty (one standard deviation, STD) is 3.3% across all participants for the total of the digit-
494 ised area (Table 3). As two glaciers (11 and 13) were not mapped by one participant, the missing val-
495 ues are replaced with the mean value from the other participants. Across all glaciers but for individual
496 participants the uncertainty (comparing the values from the four digitisation rounds) is considerably
497 lower (1% to 2.7%), indicating that the digitising is more consistent when performed by the same per-

498 son. The area values of participant 1 (P1) are systematically higher than for the other participants,
499 about 6% for the total area. A detailed analysis (close-ups and only showing individual datasets) of the
500 digitised outlines (Fig. 11) revealed that the differences are mostly due to the more generous inclusion
501 of debris-covered glacier ice for two of the larger glaciers (Nr. 1 and 5). When excluding P1, the STD
502 across the other participants is three times smaller (1.1%). The uncertainty also slightly depends on
503 glacier size, showing values between 1% and 6% for glaciers larger than 1 km² and between 2% and
504 20% for glacier <1 km². The smallest glacier in the sample is smaller than 0.1 km² and shows varia-
505 tions in STD between 8% and 44%, in the latter case also due to a reinterpretation of its extent when
506 using very high-resolution imagery. For such small glaciers related changes can thus result in consid-
507 erably different extents.

508
509 *Table 3, Figure 11*
510

511 Moreover, for P1 and most of the other participants the digitised glacier extents increased by several
512 per cent after consultation of very high resolution satellite images as available in Google Earth and
513 from the swisstopo map server (Supplement, Fig. S1). The generally very flat and debris-covered re-
514 gions were barely visible on the S2 images and have been digitised differently in each of the four
515 rounds. Hence, the possibility for a re-interpretation of the outlines within the same experiment result-
516 ed in higher standard deviations. If such regions have to be included in a glacier inventory or not can
517 be discussed, as the transition to ice-cored medial or lateral moraines is often gradual and including
518 these features in a glacier inventory or not is a (personal) methodological decision. The Figs. S2 and
519 S3 in the Supplement provide examples of the difficulties in interpreting such regions. Even at this
520 high spatial resolution the exact boundary of the two glaciers is not fully clear so that a large interpre-
521 tation spread can be expected at lower resolution. However, in general it seems that the area of glaci-
522 ers with debris-covered margins is still slightly underestimated at 10 m resolution. This confirms earli-
523 er recommendations to double-check all digitised glacier extents with such very high-resolution sen-
524 sors, at least for the difficult cases (e.g. Fischer et al. 2014).

525
526 The uncertainty (one STD) obtained with the buffer method is $\pm 5\%$ (10%) when using a 10 m (20 m)
527 buffer. Considering that the former buffer might be a realistic uncertainty bound for clean ice and the
528 latter for debris-covered ice, the ‘true’ uncertainty value would be between 5 and 10% and for individ-
529 ual glaciers largely depend on the difficulties in identifying ice under debris. This is in line with the
530 uncertainties derived from the multiple digitising and numerous previous studies.

531
532 **5.3.2 Topographic information**

533 The comparison of topographic parameters (minimum, maximum and mean elevation, mean slope and
534 aspect) revealed larger differences when derived from either the TDX or AW3D30 DEM, in particular
535 towards smaller glaciers. These are more likely to be impacted by artifacts as they share a larger per-
536 centage of their total area (Fig. 2). Differences in mean slope and aspect are generally small but in-

537 crease towards larger slope values for the former. This is in agreement with the general observations
538 that DEM quality is reduced at steep slopes. Minimum elevation is slightly higher in the TDX DEM,
539 which can be explained by glacier retreat between the acquisition dates (around 2009 for AW3D30 vs.
540 around 2013 for TDX). However, a clearly lower mean elevation due an overall surface lowering of
541 the glaciers could not be observed, indicating that the differences are in the uncertainty range. Apart
542 from artefacts, the uncorrected radar penetration of the TDX DEM into snow and firn might play a
543 role here as well.

544

545 **6. Discussion**

546 The derived size class distribution (Fig. 5) and topographic information are typical for glaciers in mid-
547 latitude mountain ranges with numerous smaller glaciers surrounding a few larger ones (e.g. Pfeffer et
548 al. 2014). Only 349 out of 4395 glaciers (8%) are larger than 1 km² and nearly one half (46%) is
549 smaller than 0.05 km² covering 2.7% of the area. It might be well possible that many of the latter are
550 no longer glaciers but just perennial snow and firn patches. However, for consistency with earlier na-
551 tional glacier inventories they have been included. Mean elevation values do not depend on size for
552 such ‘glaciers’, indicating that they can survive at different elevations and precipitation amounts have
553 a limited impact on their occurrence (e.g. if fed by avalanche snow). If they are well protected from
554 solar radiation (e.g. by shadow or debris cover) such glaciers might persist for some time despite in-
555 creasing air temperatures. Glacier mean elevation does not depend on glacier size but on glacier loca-
556 tion with respect to precipitation sources, in particular for larger glaciers (Fig. 7). On top of this de-
557 pendence is the variability with mean aspect (Fig. 7, inset).

558

559 Widespread glacier thinning over the past decades and steep terrain resulted lately in interrupted pro-
560 files for several larger valley glaciers. Their lower parts are now no longer nourished by ice from
561 above. These separated parts can thus not be named ‘regenerated glaciers’ but they melt away as dead
562 ice. Strictly speaking, such lower dead ice bodies (that can persist due to debris cover for a very long
563 time) should be excluded from a glacier inventory (Raup and Khalsa 2007). However, for consistency
564 with former inventories and their contribution to run-off we included them here and used the same ID
565 for both parts to obtain topographic information for the combined extent. Calculating this instead for
566 the individual parts would result in related outliers and a more difficult analysis of trends. At best,
567 such separated parts are identified with a flag in the attribute table, for example as a further extension
568 to the ‘Form’ attribute (e.g. ‘4: Separated glacier part’) used in the RGI (RGI consortium 2017). How-
569 ever, the differentiation from a regenerated glacier might sometimes be difficult.

570

571 Due to the differences in interpretation (Fig. 10) we have not compared the 2003 extents of individual
572 glaciers directly with those from the new inventory but only the total area of glaciers observed in both
573 inventories. Considering the underestimated glacier area in 2003 (e.g. due to missing debris cover) and

574 possibly overestimated sizes in 2015 (e.g. due to included snow) the pace of shrinkage (-1.3% /a) has
575 not changed compared to the earlier mid-1980s to 2003 period. This indicates that most glaciers have
576 not yet reached a geometry that is compliant with current climate conditions and will thus continue
577 shrinking in the future. This becomes also clear from the snow cover remaining near the end of the
578 ablation period on the glaciers, covering barely 20% to 30% of the area (e.g. Figs. 9 and 11). Assum-
579 ing a required 60% coverage of their accumulation area, glaciers in the Alps have to lose another 50%
580 to 70% of their area to reach again balanced mass budgets (Carturan et al. 2013). There are other re-
581 gions in the world with similar high (or even higher) area loss rates such as the tropical Andes (e.g.
582 Rabatel et al. 2013), but to a large extent this is also due to the smaller glaciers in this region. A realis-
583 tic comparison across regions would only be possible when change rates of identical size classes are
584 compared.

585
586 The multiple digitising experiment (Fig. 11) revealed a large variability in the interpretation of debris-
587 covered glaciers among the analysts but high consistency in the corrections where boundaries are well
588 visible. Related area uncertainties can be high for very small glaciers (>20%) but are generally <5%.
589 The here derived area reduction of about -15% since 2003 is thus significant, but for small and/or de-
590bris-covered glaciers the area uncertainty can be similar to the change, making it less reliable. Howev-
591er, this strongly depends on the specific glacier characteristics and cannot be generalized to all small
592 glaciers.

593
594 The gradual disappearance of ice under debris cover and the separation of low-lying glacier tongues
595 on steep slopes are major problems for any glacier inventory created these days. We decided to re-
596connect disconnected glacier parts by their ID (to *multi-part polygons*) for consistency with earlier
597 inventories. However, keeping them separated is another possibility, given that possible dead ice is
598 clearly marked in the attribute table.

599

600 **7. Conclusions**

601 We presented the results of a new glacier inventory for the entire Alps derived from Sentinel-2 images
602 of 2015 and 2016. In total, 4395 glaciers >0.01 km² covering an area of 1806 ±60 km² are mapped.
603 This is a reduction of about 300 km² or -15% (-1.3%/a) compared to the previous Alpine-wide inven-
604 tory from 2003. The pace of glacier shrinkage in the Alps remained about the same since the mid-
605 1980's, indicating that glaciers will continue to shrink under current climatic conditions. Due to the
606 differences in interpretation, we have not performed a glacier-by-glacier comparison of area changes.
607 The on-going glacier decline also results in increasingly difficult glacier identification (under debris
608 cover) and topologic challenges for a database (when glaciers split). The former is confirmed by the
609 results of the uncertainty assessment, showing a large variability in the interpretation of glacier extents
610 when conditions are challenging. Despite the additional workload, we think this is the best way to pro-

611 vide an uncertainty value for such a highly corrected and merged dataset. In any case, the outlines
612 from the new inventory should be more accurate than for 2003, as we here used the previous, high-
613 quality national inventories as a guide for interpretation, performed corrections by the respective ex-
614 perts, and worked with the higher resolution of Sentinel-2 data that helped in identifying important
615 spatial details.

616
617 The clean-ice mapping with the band ratio method is straightforward, but requires well-thought deci-
618 sions on the two thresholds as they will always be a compromise. They should be tested in regions
619 with ice in cast shadow and selected in a way that the workload for manual corrections is minimised.
620 If a precise DEM is available, the required corrections of wrongly mapped ice in shadow can be re-
621 duced as the further pre-processing for glaciers in Austria revealed. However, reduced DEM quality
622 and illumination differences can limit the benefits of a topographic normalisation of the images. Due
623 to the artefacts in the first version of the TanDEM-X DEM, we used the ALOS AW3D30 DEM to de-
624 rive topographic information for each glacier despite the less good temporal agreement. To conclude,
625 we had datasets with a much higher spatial resolution available for this inventory compared to the
626 2003 dataset, but for several reasons (e.g. debris cover, clouds, seasonal snow) the creation of glacier
627 inventories from satellite data and a DEM remains a challenging task with high workload and expert
628 knowledge required.

629

630 **8. Data availability**

631 The dataset can be downloaded from: <https://doi.pangaea.de/10.1594/PANGAEA.909133> (Paul et al.,
632 2019).

633

634 **Author contributions**

635 FP designed the study, prepared raw glacier outlines, performed various calculations and wrote the
636 draft manuscript. PR performed most of the GIS-based calculations and the editing that was required
637 to obtain a complete dataset and change assessment (e.g. DEM mosaicking, dataset merging, drainage
638 divides, topographic attributes, satellite footprints). All authors processed, corrected and checked the
639 created glacier outlines in their country and contributed to the contents and editing of the manuscript.
640 FP, DF, JN, AR, and PR performed the multiple digitising of glacier outlines for uncertainty assess-
641 ment.

642

643 **Competing interest**

644 The authors declare that they have no conflict of interests.

645

646 **Acknowledgements**

647 This study has been performed in the framework of the project Glaciers_cci (4000109873/14/I-NB)

648 and the Copernicus Climate Change Service (C3S) that is funded by the European Union and imple-
649 mented by ECMWF. R.S. Azzoni and D.Fugazza were funded by DARA - Department for regional
650 affairs and autonomies of the Italian presidency of the council of Ministers (funding code
651 COLL_MIN15GDIOL_M) and Levissima Sanpellegrino S.P.A., (funding code LIB_VT17GDIOL).
652 For the French Alps contribution, A. Rabatel and M. Ramusovic acknowledge the *Service National*
653 *d'Observation* GLACIOCLIM (Univ. Grenoble Alpes, CNRS, IRD, IPEV, <https://glacioclim.osug.fr/>),
654 the LabEx OSUG@2020 (*Investissements d'avenir* – ANR10 LABX56), the EquipEx GEOSUD (*In-*
655 *vestissements d'avenir* – ANR-10-EQPX-20), the CNES / Kalideos Alpes and CNES / SPOT-Image
656 ISIS program #2011-513 for providing the Pléiades images and SPOTDEM from 2011, and J.P.
657 Dedieu for its involvement in the glaciological inventories of the French Alps during past decades. For
658 the Austrian Alps, G. Schwaizer and J. Nemeč acknowledge funding from the Environmental Earth
659 Observation (ENVEO) IT GmbH and the Austrian Research Promotion Agency (FFG) within the
660 ASAP9-SenSAP project (3574408). The AW3D30 DEM is provided by the Japan Aerospace Explora-
661 tion Agency (<http://www.eorc.jaxa.jp/ALOS/en/aw3d30/index.htm>) ©JAXA. Figures 3, 4, 9, 10, and
662 11 contain modified Copernicus Sentinel data (2015, 2016). The editor thanks Andrea Fischer and
663 Sam Herreid for constructive and meaningful reviews. We would also like to thank them for their con-
664 structive comments that helped in improving the clarity of the paper.

665

666 References

- 667 Auer, I., Böhm, R., Jurkovic, A., Lipa, W., Orlik, A., Potzmann, R., Schöner, W., Ungersböck, M.,
668 Matulla, C., Briffa, K., Jones, P.D., Efthymiadis, D., Brunetti, M., Nanni, T., Maugeri, M., Mercalli,
669 L., Mestre, O., Moisselin, J.-M., Begert, M., Müller-Westermeier, G., Kveton, V., Bochnicek,
670 O., Stastny, P., Lapin, M., Szalai, S., Szentimrey, T., Cegnar, T., Dolinar, M., Gajic-Capka, M.,
671 Zaninovic, K., Majstorovic, Z. and Nieplova, E.: HISTALP – historical instrumental climatological
672 surface time series of the greater Alpine region 1760-2003, *International Journal of Climatology*,
673 *27*, 17-46, 2007.
- 674 Beniston, M., Diaz, H.F., and Bradley, R.S.: Climatic change at high elevation sites: A review, *Climatic*
675 *Change*, *36*, 233-251, 1997.
- 676 Böhm, R., Auer, I., Brunetti, M., Maugeri, M., Nanni, T., and Schöner, W.: Regional temperature variability
677 in the European Alps 1760–1998 from homogenized instrumental time series, *International*
678 *Journal of Climatology*, *21*, 1779-1801, 2001.
- 679 Carturan, L., Filippi, R., Seppi, R., Gabrielli, P., Notarnicola, C., Bertoldi, L., Paul, F., Rastner, P., Cazorzi,
680 F., Dinale, R., and Dalla Fontana, G.: Area and volume loss of the glaciers in the Ortles-Cevedale
681 group (Eastern Italian Alps): Controls and imbalance of the remaining glaciers, *The Cryosphere*, *7*,
682 1339-1359, 2013.
- 683 Casty, C., Wanner, H., Luterbacher, J., Esper, J., and Böhm, R.: Temperature and precipitation variability
684 in the European Alps since 1500, *International Journal of Climatology*, *25* (14), 1855-1880,
685 2005.
- 686 Dozier, J.: Spectral signature of alpine snow cover from Landsat 5 TM, *Remote Sensing of Environment*,
687 *28*, 9-22, 1989.
- 688 Evans, I.S., and Cox, N.J.: Global variations of local asymmetry in glacier altitude: Separation of
689 north-south and east-west components, *Journal of Glaciology*, *51* (174), 469-482, 2005.
- 690 Fischer, M., Huss, M., Barboux, C., and Hoelzle, M.: The new Swiss Glacier Inventory SGI2010: Relevance
691 of using high-resolution source data in areas dominated by very small glaciers, *Arctic, Antarctic and*
692 *Alpine Research*, *46*(4), 933-945, 2014.
- 693 Fischer, A., Seiser, B., Stocker-Waldhuber, M., Mitterer, C., and Abermann, J.: Tracing glacier changes
694 in Austria from the Little Ice Age to the present using a lidar-based high-resolution glacier inventory
695 in Austria, *The Cryosphere*, *9*, 753-766, 2015.
- 696 Frei, C.: Interpolation of temperature in a mountainous region using nonlinear profiles and non-Euclidean
697 distances, *International Journal of Climatology*, *34*, 1585-1605, 2014.
- 698 Frei, C., Christensen, J.H., Déqué, M., Jacob, D., Jones, R.G., and Vidale, P.L.: Daily precipitation
699 statistics in regional climate models: Evaluation and intercomparison for the European Alps, *Journal*
700 *of Geophysical Research*, *108*(D3), 4124, doi: 10.1029/2002JD002287, 2003.
- 701 Gardent, M., Rabatel, A., Dedieu, J.-P., and Deline, P.: Multitemporal glacier inventory of the French
702 Alps from the late 1960s to the late 2000s, *Global and Planetary Change*, *120*, 24-37, 2014.
- 703 Gardner, A. S., Moholdt, G., Cogley, J. G., Wouters, B., Arendt, A. A., Wahr, J., Berthier, E., Hock,
704 R., Pfeffer, W. T., Kaser, G., Ligtenberg, S. R. M., Bolch, T., Sharp, M. J., Hagen, J. O., van den
705 Broeke, M. R., and Paul, F.: A consensus estimate of glacier contributions to sea level rise: 2003
706 to 2009, *Science*, *340* (6134), 852-857, 2013.
- 707 Kääb, A., Winsvold, S.H., Altena, B., Nuth, C., Nagler, T., and Wuite, J.: Glacier remote sensing using
708 Sentinel-2. Part I: Radiometric and geometric performance, and application to ice velocity, *Remote*
709 *Sensing*, *8*, 598, doi:10.3390/rs8070598, 2016.
- 710 Kienholz, C., Hock, R., and Arendt, A.A.: A new semi-automatic approach for dividing glacier complexes
711 into individual glaciers, *Journal of Glaciology*, *59* (217), 925-936, 2013.
- 712 Lambrecht, A., and Kuhn, M. (2007): Glacier changes in the Austrian Alps during the last three dec-

713 ades, derived from the new Austrian glacier inventory, *Annals of Glaciology* 46, 177-184, 2007.

714 Leigh, J.R., Stokes, C.R., Carr, R.J., Evans, I.S., Andreassen, L.M., and Evans, D.J.A.: Identifying and
715 mapping very small (<0.5 km²) mountain glaciers on coarse to high-resolution imagery, *Journal of*
716 *Glaciology*, 65(254), 873-888, 2019.

717 Marzeion, B., Champollion, N., Haerberli, W., Langley, K., Leclercq, P., and Paul, F.: Observation of
718 glacier mass changes on the global scale and its contribution to sea level change, *Surveys in Geo-*
719 *physics*, 38 (1), 105-130, 2017.

720 Mölg, N., Bolch, T., Rastner, P., Strozzi, T., and Paul, F.: A consistent glacier inventory for the Kara-
721 koram and Pamir region derived from Landsat data: Distribution of debris cover and mapping
722 challenges, *Earth Systems Science Data*, 10, 1807-1827, 2018.

723 Mölg, N., Bolch, T., Walter, A., and Vieli, A.: Unravelling the evolution of Zmuttgletscher and its de-
724bris cover since the end of the Little Ice Age, *The Cryosphere*, 13, 1889-1909, 2019.

725 Oerlemans, J.: Extracting a climate signal from 169 glacier records, *Science*, 308, 675- 677, 2005.

726 Ohmura, A., Kasser, P., and Funk, M.: Climate at the equilibrium line of glaciers, *Journal of Glaciolo-*
727 *gy*, 38(130), 397-411, 1992.

728 Paul, F., Kääb, A., Maisch, M., Kellenberger, T.W., and Haerberli, W.: The new remote-sensing-
729 derived Swiss glacier inventory: I. Methods, *Annals of Glaciology*, 34, 355-361, 2002.

730 Paul, F., Kääb, A., Maisch, M., Kellenberger, T.W., and Haerberli, W.: Rapid disintegration of Alpine
731 glaciers observed with satellite data, *Geophysical Research Letters*, 31, L21402, doi:
732 10.1029/2004GL020816, 2004.

733 Paul, F., Barry, R., Cogley, J.G., Frey, H., Haerberli, W., Ohmura, A., Ommanney, C.S.L, Raup, B.,
734 Rivera, A., and Zemp, M.: Recommendations for the compilation of glacier inventory data from
735 digital sources, *Annals of Glaciology*, 50 (53), 119-126, 2009.

736 Paul, F., Frey, H., and Le Bris, R.: A new glacier inventory for the European Alps from Landsat TM
737 scenes of 2003: Challenges and results, *Annals of Glaciology*, 52 (59), 144-152, 2011.

738 Paul, F., Barrand, N. E., Baumann, S., Berthier, E., Bolch, T., Casey, K., Frey, H., Joshi, S. P.,
739 Konovalov, V., Le Bris, R., Mölg, N., Nosenko, G., Nuth, C., Pope, A., Racoviteanu, A., Rastner,
740 P., Raup, B., Scharrer, K., Steffen, S., and Winsvold, S.H.: On the accuracy of glacier outlines de-
741 rived from remote sensing data, *Annals of Glaciology*, 54 (63), 171-182, 2013.

742 Paul, F., Winsvold, S.H., Kääb, A., Nagler, T., and Schwaizer, G.: Glacier remote sensing using Senti-
743 nel-2. Part II: Mapping glacier extents and surface facies, and comparison to Landsat 8. *Remote*
744 *Sensing*, 8(7), 575; doi:10.3390/rs8070575, 2016.

745 Paul, F., Bolch, T., Briggs, K., Kääb, A., McMillan, M., McNabb, R., Nagler, T., Nuth, C., Rastner, P.,
746 Strozzi, T., and Wuite, J.: Error sources and guidelines for quality assessment of glacier area, ele-
747 vation change, and velocity products derived from satellite data in the Glaciers_cci project, *Re-*
748 *mote Sensing of Environment*, 203, 256-275, 2017.

749 Paul, F., Rastner, P., Azzoni, R.S., Diolaiuti, G., Fugazza, D., Le Bris, R., Nemeč, J., Rabatel, A., Ra-
750 musovic, M., Schwaizer, G., and Smiraglia, C.: Glacier inventory for the Alps, online:
751 <https://doi.pangaea.de/10.1594/PANGAEA.909133>, 2019.

752 Pfeffer, W. T., Arendt, A.A., Bliss, A., Bolch, T., Cogley, J. G., Gardner, A. S., Hagen, J.-O., Hock,
753 R., Kaser, G., Kienholz, C., Miles, E.S., Moholdt, G., Mölg, N., Paul, F., Radic´, V., Rastner, P.,
754 Raup, B.H., Rich, J., Sharp, M.J., and the Randolph Consortium: The Randolph Glacier Inventory:
755 A globally complete inventory of glaciers, *Journal of Glaciology*, 60 (221), 537-552, 2014.

756 Rabatel, A., and 27 others: Current state of glaciers in the tropical Andes: a multi-century perspective
757 on glacier evolution and climate change, *The Cryosphere*, 7, 81-102, 2013.

758 Rabatel, A., Ceballos, J.L., Micheletti, N., Jordan, E., Braitmeier, M., Gonzales, J., Moelg, N., Mé-
759 négoz, M., Huggel, C., and Zemp, M.: Toward an imminent extinction of Colombian glaciers?,
760 *Geografiska Annaler: Series A, Physical Geography*, 100 (1), 75-95, 2018.

761 Racoviteanu, A.E, Paul, F., Raup, B., Khalsa, S.J.S., and Armstrong, R.: Challenges in glacier map-
762 ping from space: Recommendations from the Global Land Ice Measurements from Space
763 (GLIMS) initiative, *Annals of Glaciology*, 50 (53), 53-69, 2009.

764 Rastner, P., Bolch, T., Mölg, N., Machguth, H., Le Bris, R., and Paul, F.: The first complete inventory
765 of the local glaciers and ice caps on Greenland, *The Cryosphere*, 6, 1483-1495, 2012.

766 Raup, B., and Khalsa, S.J.S.: GLIMS Analysis Tutorial, 15 pp. Online at:
767 <http://www.glims.org/MapsAndDocs/guides.html>, 2007.

768 Reid, P. C., Hari, R.E., Beaugrand, G., Livingstone, D.M., Marty, C., Straile, D., Barichivich, J., Go-
769 berville, E., Adrian, R., Aono, Y., Brown, R., Foster, J., Groisman, P., Hélaouët, P., Hsu, H., Kir-
770 by, R., Knight, J., Kraberg, A., Li, J., Lo, T., Myneni, R.B., North, R.P., Pounds, J.A., Sparks, T.,
771 Stübi, R., Tian, Y., Wiltshire, K.H., Xiao, D., and Zhu, Z.: Global impacts of the 1980s regime
772 shift, *Global Change Biology*, 22(2), 682-703, 2016.

773 RGI consortium: Randolph Glacier Inventory – A Dataset of Global Glacier Outlines: Version 6.0,
774 GLIMS Technical Report, 71 pp., online at: glims.org/RGI/00_rgi60_TechnicalNote.pdf, 2017.

775 Sakai, A., Nuimura, T., Fujita, K., Takenaka, S., Nagai, H., and Lamsal, D. (2015): Climate regime of
776 Asian glaciers revealed by GAMDAM glacier inventory, *The Cryosphere*, 9, 865-880.

777 Smiraglia, C., Diolaiuti, G.A.: The new Italian glacier inventory, 1st ed., Ev-K2-CNR Publications,
778 Bergamo, 2015.

779 Smiraglia, P., Azzoni, R.S., D'Agata, C., Maragno, D., Fugazza, D., and Diolaiuti, G.A.: The evolu-
780 tion of the Italian glaciers from the previous data base to the new Italian inventory. Preliminary
781 considerations and results, *Geografia Fisica e Dinamica Quaternaria* 38, 79-87, 2015.

782 Stumpf, A., Michéa, D., and Malet, J.-P.: Improved co-registration of Sentinel-2 and Landsat-8 image-
783 ry for earth surface motion measurements, *Remote Sensing*, 10(2), 160, doi: 10.3390/rs10020160,
784 2018.

785 Takaku, J., Tadono, T., and Tsutsui, K.: Generation of high resolution global DSM from ALOS
786 PRISM, *ISPRS International Archives of the Photogrammetry, Remote Sensing and Spatial In-*
787 *formation Sciences*, Vol. XL-4, 243-248, 2014.

788 Vaughan, D. G., Comiso, J. C., Allison, I., Carrasco, J., Kaser, G., Kwok, R., Mote, P., Murray, T.,
789 Paul, F., Ren, J., Rig- not, E., Solomina, O., Steffen, K., and Zhang, T.: Observations: Cryosphere,
790 in: *Climate Change 2013: Physical Science Basis. Contribution of Working Group I to the Fifth*
791 *Assessment Report of the Intergovernmental Panel on Climate Change*, edited by: Stocker, T. F.,
792 Qin, D., Plattner, G.-K., Tignor, M., Allen, S. K., Boschung, J., Nauels, A., Xia, Y., Bex, V., and
793 Midgley, P. M., Cambridge University Press, Cambridge, United Kingdom and New York, NY,
794 USA, 317-382, 2013.

795 Wouters, B., Gardner, A.S., and Moholdt, G.: Global glacier mass loss during the GRACE satellite
796 mission (2002-2016), *Frontiers in Earth Science*, 7 (96), doi: 10.3389/feart.2019.00096, 2019.

797 Zemp, M., Hoelzle, M., and Haeberli, W.: Distributed modelling of the regional climatic equilibrium
798 line altitude of glaciers in the European Alps, *Global and Planetary Change*, 56, 83–100, 2007.

799 Zemp, M., Paul, F., Hoelzle, M., and Haeberli, W.: Alpine glacier fluctuations 1850-2000: An over-
800 view and spatio-temporal analysis of available data and its representativity. In: Orlove, B., Wie-
801 gandt, E. and Luckman, B. (eds.): *Darkening Peaks: Glacier Retreat, Science, and Society*, Univer-
802 sity of California Press, Berkeley and Los Angeles, 152-167, 2008.

803 Zemp, M., Frey, H., Gärtner-Roer, I., Nussbaumer, S.U., Hoelzle, M., Paul, F., Haeberli, W., Den-
804 zinger, F., Ahlstrom, A.P., Anderson, B., Bajracharya, S., Baroni, C., Braun, L.N., Caceres, B.E.,
805 Casassa, G., Cobos, G., Davila, L.R., Delgado Granados, H., Demuth, M.N., Espizua, L., Fischer,
806 A., Fujita, K., Gadek, B., Ghazanfar, A., Hagen, J.O., Holmlund, P., Karimi, N., Li, Z., Pelto, M.,
807 Pitte, P., Popovnin, V.V., Portocarrero, C.A., Prinz, R., Sangewar, C.V., Severskiy, I., Sigurdsson,
808 O., Soruco, A., Usubaliev, R., and Vincent, C.: Historically unprecedented global glacier changes

809 in the early 21st century, *Journal of Glaciology*, 61 (228),745-762, 2015.
810 Zemp, M., Huss, M., Thibert, E., Eckert, N., McNabb, R., Huber, J., Barandun, M., Machguth, H.,
811 Nussbaumer, S.U., Gärtner-Roer, I., Thomson, L., Paul, F., Maussion, F., Kutuzov, S., and
812 Cogley, J.G.: Global glacier mass changes and their contributions to sea-level rise from 1961 to
813 2016, *Nature*, 568, 382-386, 2019.
814

815 **Tables**

816 *Table 1: Details about the Sentinel-2 tiles used to create the inventory, C.: Country.*

Nr.	Tile	Date	C.	Nr.	Tile	Date	C.	Nr.	Tile	Date	C.
1	32TMT	29 8 15	CH	11	32TNS	26 8 15	CH	21	31TGL	29 8 15	FR
2	32TNT	29 8 15	CH	12	32TNS	29 9 16	IT	22	32TLR	29 8 15	FR
3	32TNT	26 8 15	AT	13	32TNS	29 9 16	AT	23	32TLR	29 8 15	CH
4	32TPT	26 8 15	AT	14	32TPS	26 8 15	AT	24	32TLR	29 8 15	IT
5	32TQT	27 8 16	AT	15	32TPS	29 9 16	IT	25	32TLR	7 10 17	IT
6	33TUN	27 8 16	AT	16	32TPT	26 9 16	IT	26	32TMR	7 10 17	IT
7	32TLS	29 8 15	CH	17	32TQT	27 8 16	IT	27	31TGK	29 8 15	FR
8	32TLS	29 8 15	FR	18	32TQS	7 8 16	IT	28	32TLQ	23 8 16	IT
9	32TMS	29 8 15	CH	19	32TQS	27 8 16	AT	29	32TLP	29 8 15	IT
10	32TMS	23 8 16	IT	20	33TUM	2 8 17	IT				

817

818

819 *Table 2: Glacier area and count per size class for the entire sample.*

Size class [km ²]	0.01- 0.02	0.02- 0.05	0.05- 0.1	0.1- 0.2	0.2- 0.5	0.5-1	1-2	2-5	5-10	10-20	>20	All
Count	966	1060	723	533	520	244	177	103	48	16	5	4395
Count [%]	22.0	24.1	16.5	12.1	11.8	5.6	4.0	2.3	1.1	0.4	0.1	100
Area [km ²]	13.83	34.44	51.42	75.48	163.87	168.28	249.06	319.13	322.96	211.85	195.56	1805.9
Area [%]	0.8	1.9	2.8	4.2	9.1	9.3	13.8	17.7	17.9	11.7	10.8	100

820

821

822 *Table 3: Results of the multiple digitising experiment, listing for each of the five participants*
 823 *the mean glacier area (in km²) in the columns P1 to P5 along with the standard deviation in*
 824 *per cent (STD%). The last two columns provide the averaged values across all participants*
 825 *for each glacier and the last row gives total areas and their standard deviation across all*
 826 *glaciers and for each participant. The two values marked in blue are mean values derived*
 827 *from the other four participants. Red values mark highest values for glaciers larger and*
 828 *smaller than 1 km². Glacier ID 4 is missing as it was digitised as one glacier (with ID 5) by*
 829 *most participants.*

Gl.-ID	P1	STD%	P2	STD%	P3	STD%	P4	STD%	P5	STD%	Mean	STD%
1	9.37	1.89	8.96	0.18	8.40	0.79	8.77	0.99	8.64	3.86	8.83	4.14
2	6.50	2.10	6.08	1.31	6.07	1.43	5.95	0.81	6.25	1.31	6.17	3.48
3	0.79	3.75	0.72	3.51	0.65	1.62	0.73	0.74	0.71	8.77	0.72	7.02
5	4.10	3.03	3.22	2.33	3.50	3.92	3.45	5.66	3.45	7.46	3.54	9.33
6	2.88	1.82	2.83	1.52	2.90	3.32	2.75	2.69	2.91	1.86	2.85	2.27
7	1.20	1.04	1.06	6.10	1.16	2.71	1.14	1.91	1.20	2.90	1.15	4.81
8	5.35	0.24	5.13	1.58	5.25	0.77	5.24	0.31	5.26	1.24	5.25	1.51
9	2.75	0.43	2.75	1.64	2.59	3.80	2.72	2.17	2.64	1.53	2.69	2.64
10	0.38	6.38	0.30	2.76	0.25	4.37	0.30	3.39	0.25	4.80	0.30	17.24
11	0.28	12.40	0.27	0.64	0.26	2.06	0.26	1.71	0.30	8.69	0.27	6.77
12	0.24	1.41	0.25	4.34	0.20	3.30	0.21	5.54	0.23	6.79	0.23	8.85
13	0.08	41.67	0.12	17.80	0.03	8.00	0.08	17.68	0.11	17.65	0.08	44.21
14	0.21	4.29	0.17	15.52	0.11	16.16	0.20	5.03	0.21	13.42	0.18	24.01
15	0.12	4.96	0.12	7.10	0.11	1.09	0.11	14.22	0.14	3.45	0.12	11.01
Sum	34.25	1.48	31.97	0.97	31.48	1.13	31.90	0.91	32.31	2.72	32.38	3.35

830

831

832 **Figure captions**

833 Fig. 1: Overview of the study region with footprints (colour-coded for acquisition year) of the Senti-
834 nel-2 tiles used (see Table 1 for numbers).

835

836 Fig. 2: Comparison of hillshade views from a) the AW3D30 DEM and b) the TanDEM-X DEM for a
837 region around the Mt. Blanc/Monte Bianco. Glacier outlines are shown in red, data voids in the Tan-
838 DEM-X DEM are depicted as constantly grey areas. The yellow circle marks the Mt. Blanc summit,
839 the yellow cross in the lower centre marks the coordinates 45.8° N and 6.9° E. The AW3D30 DEM
840 has been obtained from <https://www.eorc.jaxa.jp/ALOS/en/aw3d30/index.htm> and is provided by
841 JAXA. The TanDEM-X DEM has been acquired by the TerraSAR-X/TanDEM-X mission and is pro-
842 vided by DLR (DEM_GLAC1823).

843

844 Fig. 3: Results of the automated (clean ice) glacier mapping and threshold selection. a) band ratio MSI
845 band 4 / MSI band 11 (red/SWIR). b) Glacier classification results using different thresholds. The
846 lower values add some additional pixels, in particular in shadow regions where the threshold is most
847 sensitive. c) Blue band threshold to remove wrongly classified rock in shadow. The highest value has
848 been used resulting in a good performance in the left part of the image (white arrow) and a bad one to
849 the right (green arrow), where correctly classified ice in shadow is removed. d) Final outlines (light
850 blue) on top of the Sentinel-2 image in natural colours. The yellow cross to the lower right of the cen-
851 tre of panel a) is marking the coordinates 45.87° N and 7.0° E. Sentinel-2 image source: Copernicus
852 Sentinel data (2015).

853

854 Fig. 4: Examples of challenging classifications in different countries. a) Debris cover delineation (red)
855 around Grossvenediger (Hohe Tauern) in Austria with raw extents (light grey) and outlines from the
856 previous national inventory (yellow). b) Tré-La-Tête Glacier (Mont-Blanc) with automatically derived
857 glacier extents (green), manually corrected outlines from 2015 (red) and outlines derived from aerial
858 photographs taken in 2008 (yellow). The S2 image from August 2015 is in the background. c) Subset
859 of the Orobic Alps in Italy (S2 image from September 2016), with evidence of topographic shadow
860 and debris covered glaciers. The inset shows an aerial photograph with better glacier visibility but sea-
861 sonal snow. d) S2 image from 2015 showing differences in interpretation of debris cover for Gavirolas
862 glacier in Switzerland for the inventories from 2003 (yellow), 2008 (green) and 2015 (red). The inset
863 shows a close-up of its lowest debris-covered part obtained from aerial photography for comparison
864 (this image is a screenshot from Google Earth). The yellow crosses in each panel mark the following
865 geographic coordinates: a) 47.12° N, 12.4° E; b) 45.8° N, 6.75° E; c) 46.09° N, 10.07° E; d) 46.86° N,
866 9.06° E. Source of all Sentinel-2 images shown in the background: Copernicus Sentinel data (2015 and
867 2016).

868

869 Fig. 5: Relative frequency histograms for glacier count and area per a) size class and b) aspect sector
870 for all glaciers.

871

872 Fig. 6: Glacier area vs. a) minimum and maximum elevation and b) elevation range for all glaciers.

873

874 Fig. 7: Spatial distribution of median elevation (colour coded) for glaciers larger 0.5 km². The inset
875 shows a scatterplot depicting glacier aspect (counted from North at 0/360°) vs. median elevation and
876 values averaged for each cardinal direction.

877

878 Fig. 8: Normalised glacier hypsometry per country as derived from the AW3D30 DEM.

879

880 Fig. 9: Visualisation of the strong glacier area shrinkage between 2003 (yellow) and 2015 (red) for a
881 sub-region of the Zillertal Alps (Austria and Italy). The yellow cross in the middle right is marking the
882 coordinates 47.0° N and 11.88° E. Sentinel-2 image source: Copernicus Sentinel data (2016).

883

884 Fig. 10: Overlay of glacier outlines from 2003 (black) and 2016 (yellow) showing the different inter-
885 pretation of glacier extents for the region around Sonnblickkees (SBK) in Austria. The black cross in
886 the lower right is marking the coordinates 47.12° N and 12.6° E. Sentinel-2 image source: Copernicus
887 Sentinel data (2016).

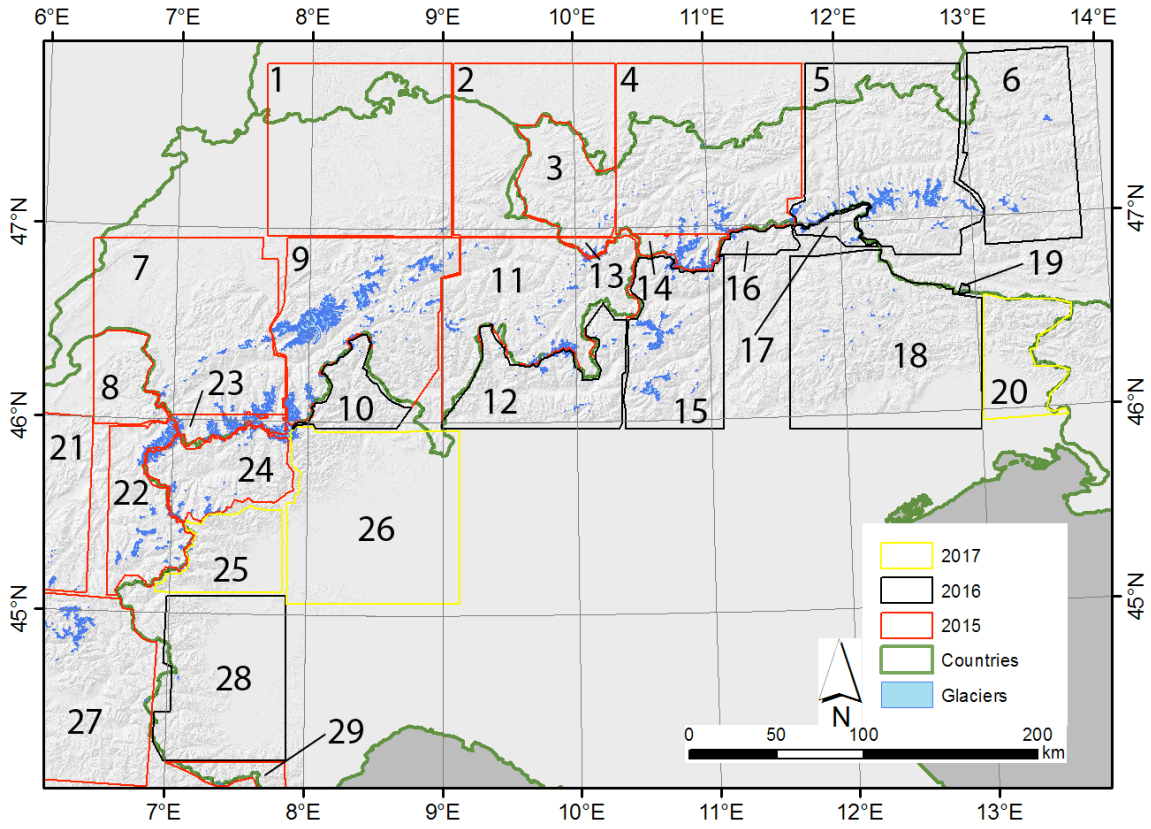
888

889 Fig. 11: Overlay of glacier outlines from the multiple digitising experiment by all participants. Colours
890 refer to the first (yellow), second (red), third (green) and fourth (white) round of digitisation. The
891 white cross in the upper right is marking the coordinates 46.0° N and 7.5° E. Sentinel-2 image source:
892 Copernicus Sentinel data (2015).

893

894

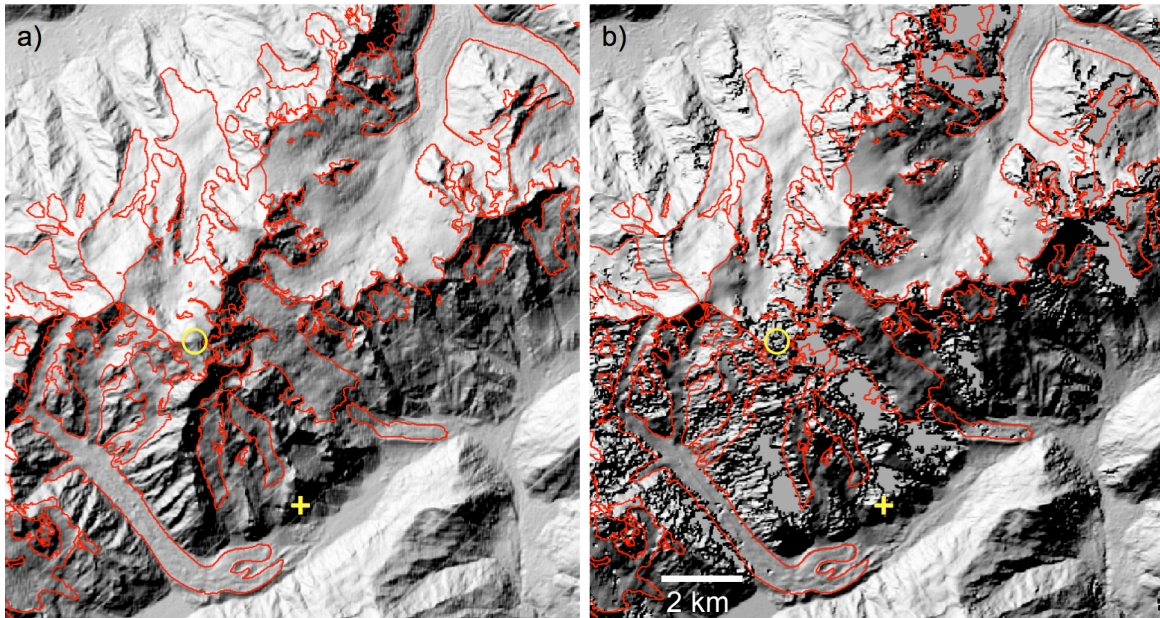
895 **Figures**



896

897 Figure 1

898



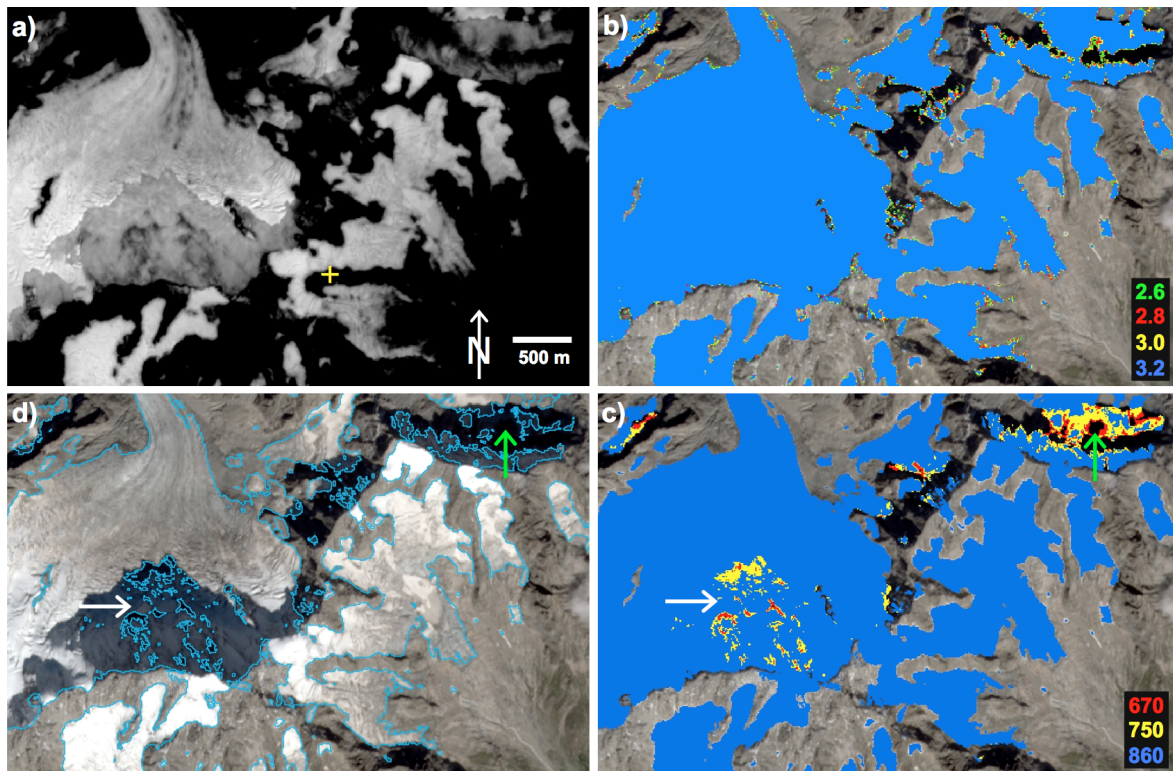
899

900 Figure 2

901

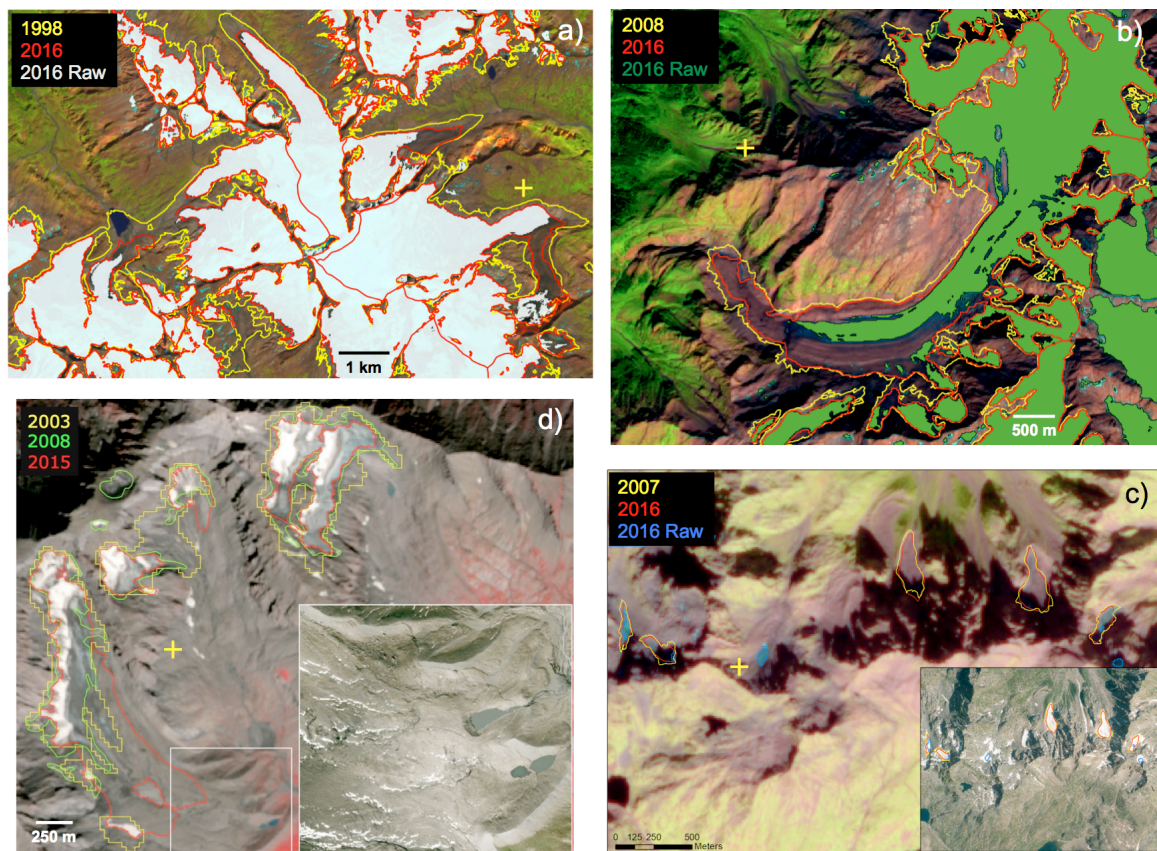
902

903



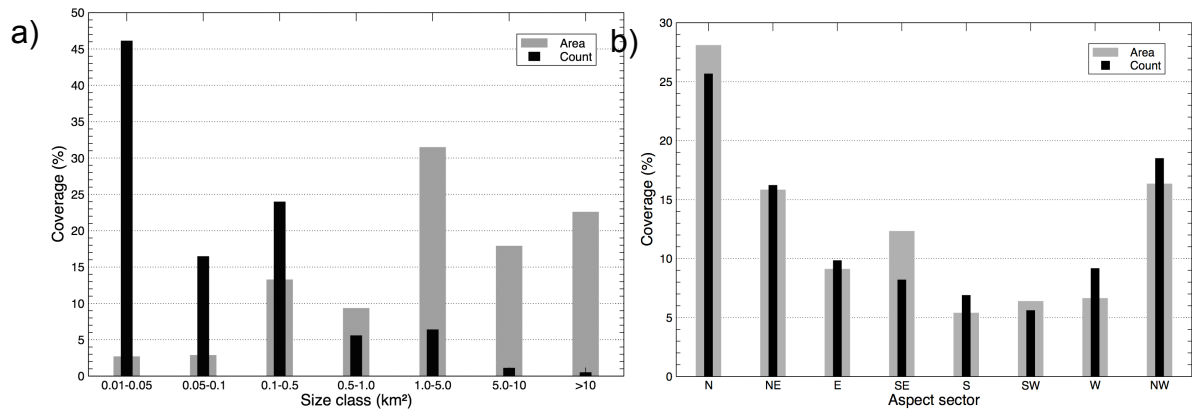
904
905
906
907

Figure 3



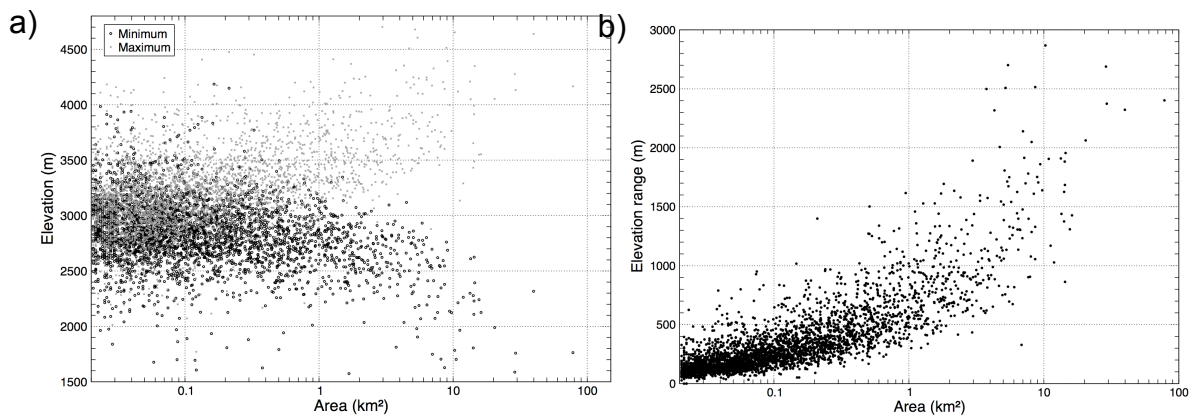
908
909
910
911

Figure 4



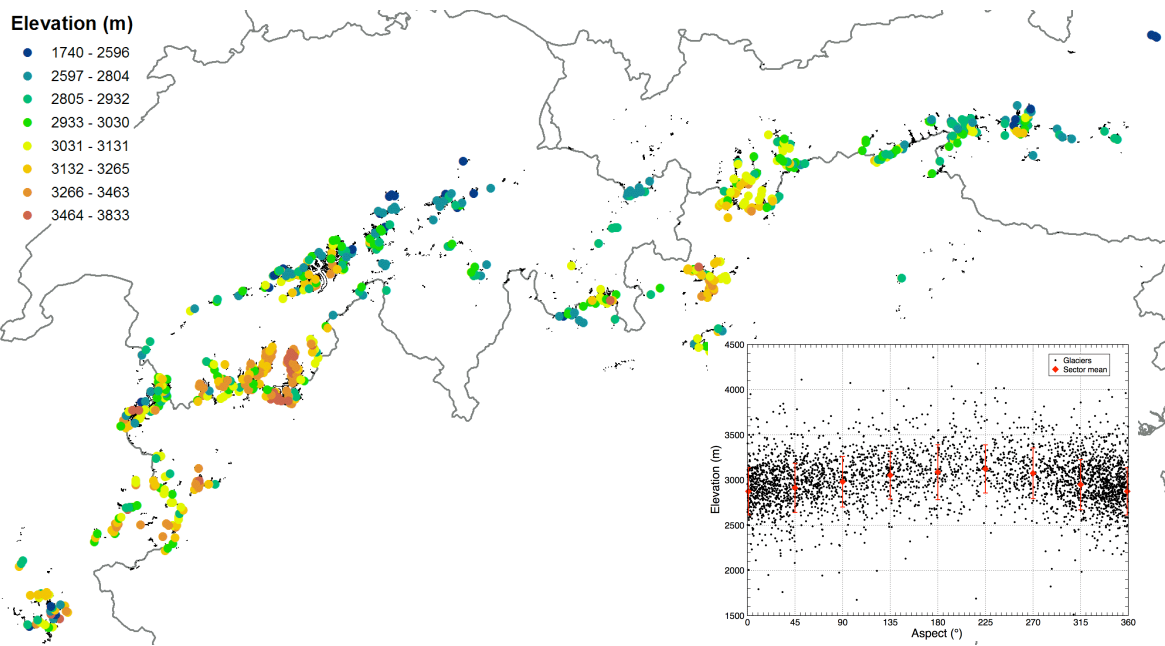
912
913 Figure 5

914
915



916
917 Figure 6:

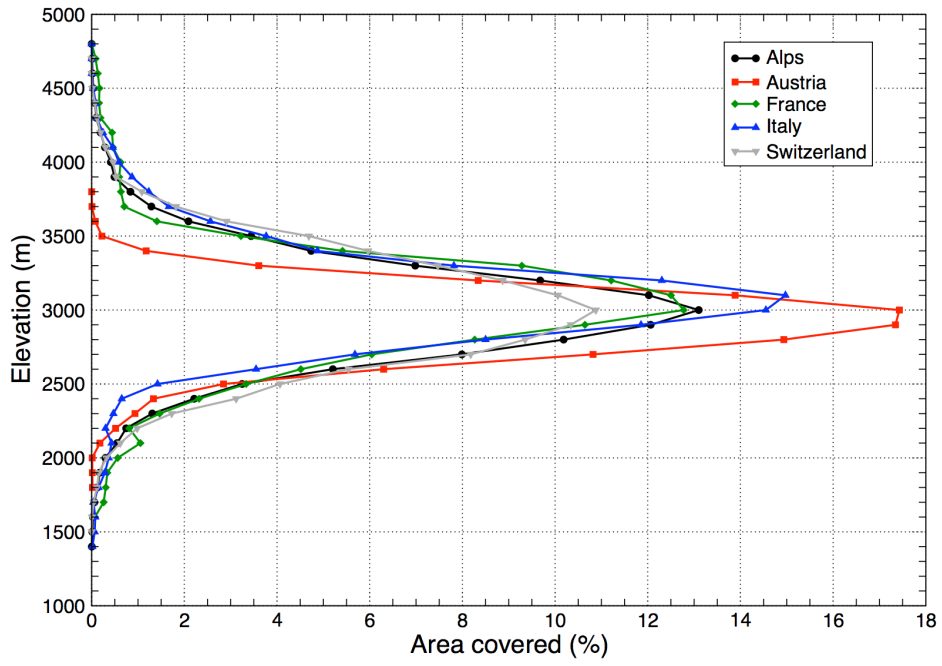
918
919



920
921 Figure 7

922
923

924

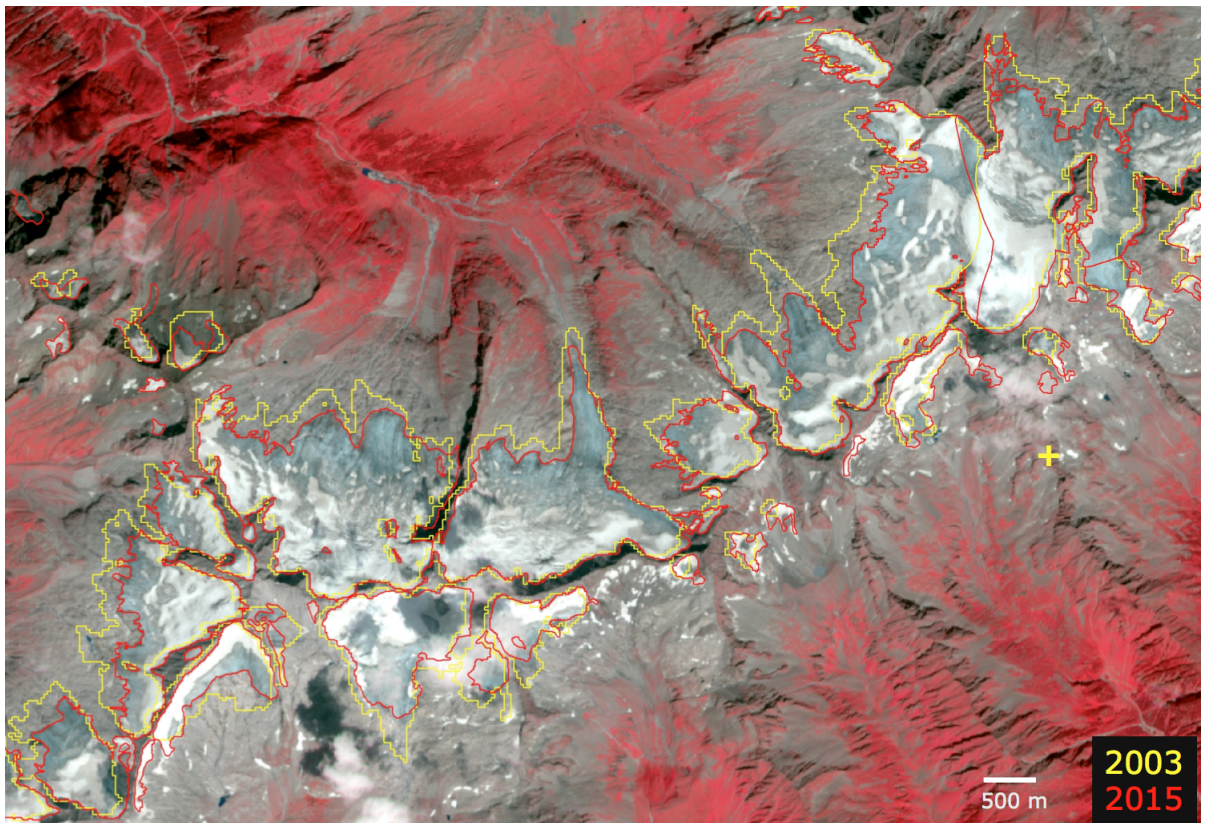


925

926 Figure 8

927

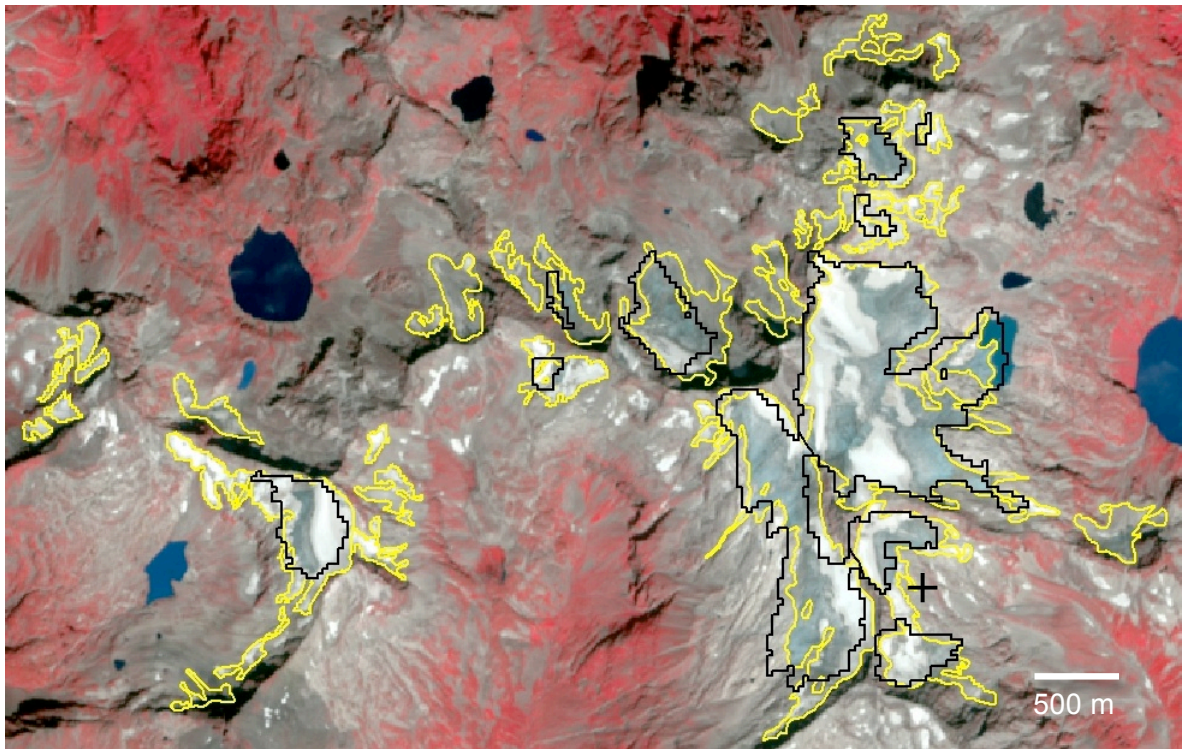
928



929

930 Figure 9

931

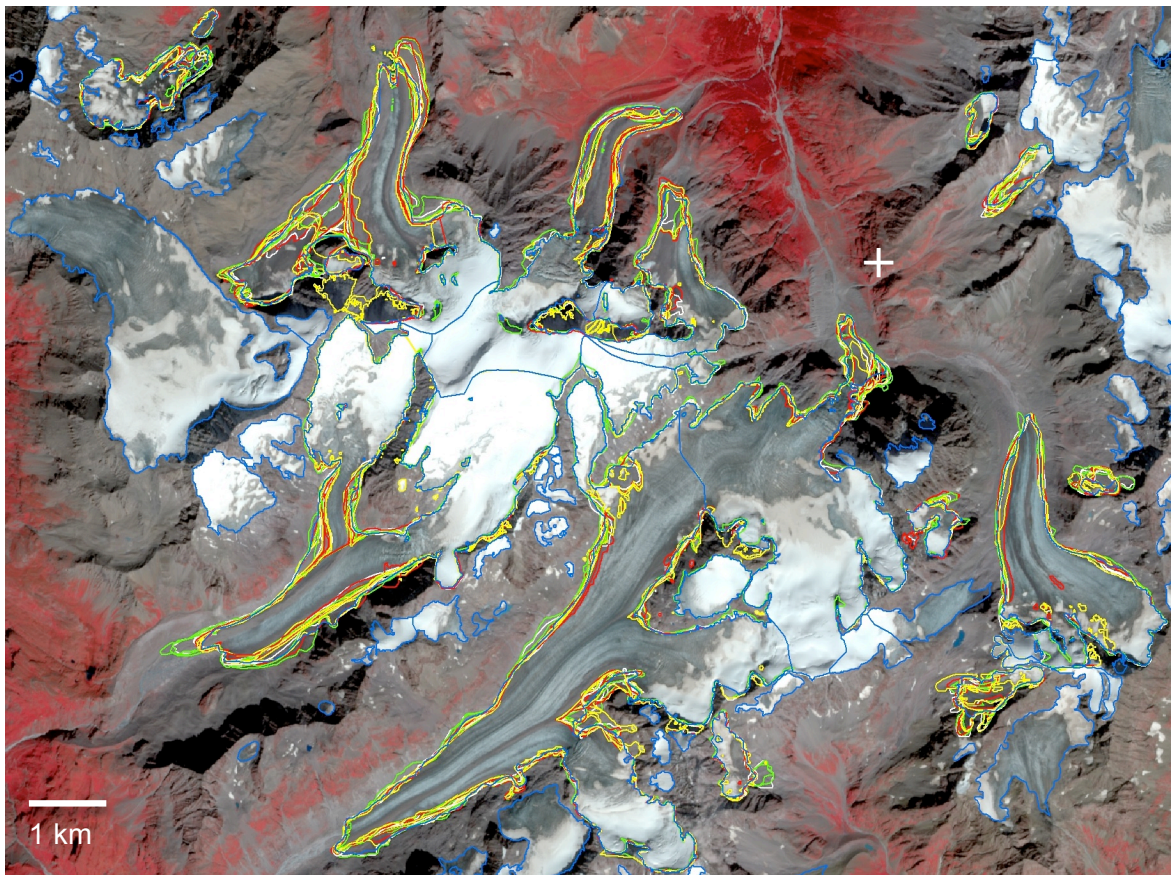


932

933 Figure 10

934

935



936

937 Figure 11

938